SRTTU

JCARME
ISSN: 2228-7922
Journal of Computational and Applied Research in Mechanical Engineering
Vol. 8, No. 1, pp. 25-38
jcarme.sru.ac.ir

Three-dimensional boundary layer flow and heat transfer of a dusty fluid towards a stretching sheet with convective boundary conditions

B. C. Prasannakumara[a,*], N. S. Shashikumar[a] and M. Archana[b]

[a]Government First Grade College, Koppa, Chikkamagaluru-577126, Karnataka, India
[b]Department of Studies and Research in Mathematics, Kuvempu University, Shankaraghatta-577451, Shimoga, Karnataka, India

Article info:
Received: 80/03/2017
Accepted: 02/12/2017
Online: 10/04/2018

Keywords:
Dusty fluid,
Convective boundary condition,
Stretching sheet,
Runge-Kutta-Fehlberg 45 method.

Abstract
The steady three-dimensional boundary layer flow and heat transfer of a dusty fluid towards a stretching sheet with convective boundary conditions are investigated using similarity solution approach. The free stream along z-direction impinges on the stretching sheet to produce a flow with different velocity components. The governing equations are reduced into ordinary differential equations using appropriate similarity variables. Reduced nonlinear ordinary differential equations subjected to the associated boundary conditions are solved numerically using Runge–Kutta fourth-fifth order method along with shooting technique. The effects of the physical parameters like magnetic parameter, velocity ratio, fluid and thermal particle interaction parameter, Prandtl number, Eckert number and Biot number on flow and heat characteristics are examined, illustrated graphically, and discussed in detail. The results indicate that the fluid phase velocity is always greater than that of the particle phase and temperature profiles of the fluid and dust phases increase with the increase of the Eckert number.

Nomenclature

$\mathrm{B_i}$	Biot number
(x, y)	Cartesian coordinates $[m]$
h_f	Convective heat transfer coefficient
$\mathrm{Ec_x}, \mathrm{Ec_y}$	Eckert numbers
Nu	Local Nusselt number
M	Magnetic parameter
Pr	Prandtl number
$\mathrm{Cf_x}, \mathrm{Cf_y}$	Skin friction coefficients
c_m	Specific heat of dust fluid $[m^2 s^{-2} K^{-1}]$
c_p	Specific heat of fluid $[m^2 s^{-2} K^{-1}]$
B_0	Strength of applied magnetic field
c	Stretching rate
u_w, v_w	Stretching velocities along x and y directions
$\mathrm{q_w}$	Surface heat transfer rate
T_f	Temperature at the wall $[K]$
T_p	Temperature of the dust phase $[K]$
T	Temperature of the fluid $[K]$
T_∞	Temprature at large distance from the wall $[K]$
k	Thermal conductivity $[kgms^{-3}K^{-1}]$
(u_p, v_p, w_p)	Velocity component of the dusty fluid along x, y and z directions $[ms^{-1}]$

(u, v, w)	Velocity component of the fluid along x, y and z directions $[ms^{-1}]$
Greek symbols	
ρ, ρ_p	Density of the fluid and dust phase
ω	Density ratio
η	Dimensionless space variable
θ_p	Dust phase temperature
μ	Dynamic viscosity $[kgm^{-1}s^{-1}]$
σ	Electric conductivity
θ	Fluid phase temperature
β_T	Fluid-particle interaction parameter for temperature
β	Fluid-particle interaction parameter
ν	Kinematic viscosity$[m^2s^{-1}]$
λ	Ratio of the velocities in y- and x-directions
ρ_r	Relative density$[kgm^{-3}]$
τ_v	Relaxation time of the of dust particle
α	Thermal diffusivity
τ_T	Thermal equilibrium time
τ_{zx}, τ_{zy}	Wall shear stress
Subscripts	
p	Dust phase
Superscript	
$'$	Derivative with respect to η

1. Introduction

Analysis of boundary layer flow and heat transfer over a stretching surface have many engineering applications in industrial processes such as polymer industry involving cooling of a molten liquid, paper production, rolling and manufacturing of sheets and fibers, drawing of plastic film etc. Particularly the study of the flow of dusty fluid has important applications in the field of cooling systems, centrifugal fields of cooling systems, centrifugal separation of matter from a fluid, petroleum industry, and purification of crude oil, polymer technology, and fluid droplets spray. One of the pioneering studies in this field was conducted by Sakiadis [1] who presented boundary layer flow behavior over a continuous solid surface moving with constant speed. The flow of an incompressible viscous fluid over a linearly stretching sheet was studied by Crane [2] who obtained an exact solution for the flow field. Liu et al. [3] analyzed the laminar boundary-layer flow and heat transfer for three-dimensional viscous fluid driven by a horizontal the exponentially stretching surface in two lateral directions. Hayat et al. [4] investigated the three-dimensional boundary layer flow of Eyring Powell nanofluid in the presence of exponentially stretching sheet. Nadeem et al. [5] discussed the MHD three-dimensional boundary layer flow of Casson nanofluid over a linearly stretching surface with convective boundary condition. An unsteady MHD laminar nanofluid regime over a porous accelerating stretching surface in a water based incompressible nanofluid containing different types of nanoparticle was studied by Abolbashari et al. [6]. Freidoonimehr et al. [7] investigated the transient MHD laminar free convection flow of nanofluid past a vertical surface. The steady of boundary layer flow and heat transfer over a stretching surface in rotating fluid were examined by Butt et al. [8]. The three-dimensional boundary layer flow of a nanofluid over an elastic sheet stretched nonlinearly in two lateral directions was examined by Khan et al. [9]. Shehzad et al. [10] addressed the convective heat and mass conditions in steady 3-D flow of an incompressible Oldroyd-B nanofluid over a radiative surface. Laminar three-dimensional flow and entropy generation in a nanofluid filled cavity with triangular solid insert at the corners was analyzed by Kolsi et al. [11]. Hayat et al. [12] observed that the effects of Brownian motion parameter and thermophoresis parameter on the nanoparticles concentration distribution were quite opposite. Recently, Hayat et al. [13] analyzed the effects of inclined magnetic field and Joule heating in three-dimensional boundary layer flow of an incompressible viscous fluid by an unsteady exponentially stretched surface embedded in a thermally stratified medium.

In the all above cited papers, the considered fluid was incompressible, viscous and free from impurities. But, in nature, the fluid in pure form is rarely available. Water and air contain impurities like dust particles and foreign bodies. In recent years, researchers have turned to study dusty fluid. Study of boundary layer flow and heat transfer in dusty fluid is very constructive in understanding of various industrial and engineering problems concerned with atmospheric fallout, powder technology, rain erosion in guided missiles, sedimentation, combustion, fluidization, nuclear reactor

cooling, electrostatic precipitation of dust, wastewater treatment, acoustics batch settling, lunar ash flows aerosol, and paint spraying, and etc.

In the past few decades, researchers have focused on analyzing the heat and mass transfer characteristics of dusty fluid through different channels. Fundamental studies in dynamics of dusty fluid, its behavior and boundary layer modeling were studied by Saffman [14], Chakrabarti [15] and Datta et al. [16]. The effect of temperature-dependent thermal conductivity and viscosity on unsteady MHD Couette flow and heat transfer of viscous dusty fluid between two parallel plates were investigated by Mosayebidorcheh et al. [17]. Prakash et al. [18] examined the combined effects of thermal radiation, buoyancy force and magnetic field on heat transfer of MHD oscillatory dusty fluid flow through a vertical channel filled with a porous medium. Unsteady Couette flow of a dusty viscous incompressible electrically conducting fluid through porous media with heat transfer was studied by Attia et al. [19], with the consideration of both Hall current and ion slip effect. Muthuraj et al. [20] investigated the influence of elasticity of flexible walls on the MHD peristaltic transport of a dusty fluid with heat and mass transfer in a horizontal channel in the presence of chemical reaction under a long wavelength approximation. Effects of variable viscosity and thermal conductivity on magnetohydrodynamic flow and heat transfer of a dusty fluid over an unsteady stretching sheet were analyzed numerically by Manjunatha et al. [21]. The steady three-dimensional, incompressible, laminar boundary layer stagnation point flow and heat transfer of a dusty fluid towards a stretching sheet were investigated by Mohaghegh et al. [22] using similarity solution approach. Further, many authors [23-27] have been studied flow and heat transfer phenomena of dusty fluid under different geometries by considering various effects.

In recent years, heat transfer due to convective surface over various geometries has received considerable attention for its potential applications in several engineering and industrial processes like transpiration cooling process, material drying, etc. The use of convective boundary condition at the surface of the body is more general and realistic to apply. Bataller [28] investigated the effects of radiation on the Blasius and Sakiadis flows with convective boundary condition. Aziz [29] studied heat transfer problems for the boundary layer flow concerning a convective boundary condition and established the condition in which the convection heat transfer coefficient must satisfy the existence of similarity solution. Makinde [30] extended the work of Aziz [29] by including hydromagnetic field and mixed convection heat and mass transfer over a vertical flat plate. Merkin and Pop [31] studied the forced convection heat transfer resulting from the flow of a uniform stream over a flat surface on which there was a convective boundary condition. Apart from these works, various aspects of flow and heat transfer over a stretching surface with convective boundary condition were investigated by many researchers [32-37].

The present study investigates the dusty fluid behavior on three-dimensional boundary layer flow and heat transfer over a stretching sheet with convective boundary condition. Appropriate similarity transformations are used to reduce the governing partial differential equations into a set of nonlinear ordinary differential equations. The resulting equations are solved numerically using Runge–Kutta Fehlberg fourth-fifth order method with the help of shooting technique. The effect of variations of several pertinent emerging parameters on the flow and heat transfer characteristics is analyzed in detail.

2. Formulation

Consider a steady three-dimensional flow of an incompressible boundary layer flow of dusty fluid over a horizontal stretching surface. It is assumed that the sheet is stretched along the xy-plane, while fluid is placed along the z-axis. The particles are taken to be small enough and of sufficient number and are treated as a continuum which allow concepts such as density and velocity to have physical meaning. Moreover, it is also considered that the constant magnetic field B_0 is applied normal to the fluid flow and

the induced magnetic field is assumed to be negligible. The flow region is confined to $z > 0$, and the sheet is assumed to stretch with the linear velocities $u_w = c\lambda x$ and $v_w = cy$ along the xy-plane, respectively, where c is the stretching rate and λ is the coefficient which indicate the difference between the sheet velocity components in x and y directions. The dust particles are treated as spheres with uniform size, and their density is taken constant throughout the flow. Here both phases behave as a viscous fluid, and the volume fraction of suspended particles is finite and constant.

The coordinate system and flow regime are illustrated in Fig. 1. The boundary layer equations of 3-D incompressible dusty fluid are stated as:

$$u\frac{\partial u}{\partial x} + v\frac{\partial u}{\partial y} + w\frac{\partial u}{\partial z} = \nu\left(\frac{\partial^2 u}{\partial x^2} + \frac{\partial^2 u}{\partial y^2} + \frac{\partial^2 u}{\partial z^2}\right) + \frac{\rho_p}{\rho\tau_v}(u_p - u) - \sigma\frac{\beta_0^2}{\rho_\tau}u, \quad (1)$$

$$u\frac{\partial v}{\partial x} + v\frac{\partial v}{\partial y} + w\frac{\partial v}{\partial z} = \nu\left(\frac{\partial^2 v}{\partial x^2} + \frac{\partial^2 v}{\partial y^2} + \frac{\partial^2 v}{\partial z^2}\right) + \frac{\rho_p}{\rho\tau_v}(v_p - v) - \sigma\frac{\beta_0^2}{\rho_\tau}v, \quad (2)$$

$$u_p\frac{\partial u_p}{\partial x} + v_p\frac{\partial u_p}{\partial y} + w_p\frac{\partial u_p}{\partial z} = \frac{1}{\tau_v}(u - u_p), \quad (3)$$

$$u_p\frac{\partial v_p}{\partial x} + v_p\frac{\partial v_p}{\partial y} + w_p\frac{\partial v_p}{\partial z} = \frac{1}{\tau_v}(v - v_p), \quad (4)$$

$$u_p\frac{\partial w_p}{\partial x} + v_p\frac{\partial w_p}{\partial y} + w_p\frac{\partial w_p}{\partial z} = \frac{1}{\tau_v}(w - w_p), \quad (5)$$

$$u\frac{\partial T}{\partial x} + v\frac{\partial T}{\partial y} + w\frac{\partial T}{\partial z} = \alpha\frac{\partial^2 T}{\partial z^2} + \frac{\rho_p}{\rho}\frac{T_p - T}{\tau_T} + \frac{\rho_p}{\rho c_p}\frac{1}{\tau_v}\left[(u_p - u)^2 + (v_p - v)^2\right], \quad (6)$$

$$u_p\frac{\partial T_p}{\partial x} + v_p\frac{\partial T_p}{\partial y} + w_p\frac{\partial T_p}{\partial z} = \frac{c_p}{c_m}\frac{T_p - T}{\tau_T}, \quad (7)$$

with boundary conditions as:

$$u = u_w, v = v_w, w = 0, -k\frac{\partial T}{\partial y} = h_f(T_f - T) \text{ at } z = 0 \quad (8)$$

$$u_p = u = 0, v_p = v = 0, w_p = w, \rho_p = \rho\omega, T = T_\infty, T_p = T_\infty \quad \text{at} \quad z \to \infty \quad (9)$$

where (u, v, w) and (u_p, v_p, w_p) denote the velocity components of the fluid and dust phases in the $x-, y-$, and $z-$directions, respectively. ρ and ρ_p are the densities of fluid and dust phases, respectively. α, ν, σ, c_p and c_m are thermal diffusivity, kinematic viscosity, electric conductivity, specific heat of the fluid and dust phases, respectively. τ_T is the thermal equilibrium time i.e., the time required by the dust cloud to adjust its temperature to the fluid, τ_v is the relaxation time of the of dust particle i.e., the time required by a dust particle to adjust its velocity relative to the fluid. Throughout the study, it is assumed that $c_p = c_m$. In Eq. (6 and 7), T and T_p represent the temperatures of the fluid and dust particles inside the boundary layer respectively. In deriving these equations, the drag force is considered for the interaction between the fluid and particle phases. In the expressions of Eq. (8-9), u_w and v_w are the stretching velocities along x and y directions, respectively, h_f is the convective heat transfer coefficient, T_f is the convective fluid temperature below the moving sheet, and k is the thermal conductivity.

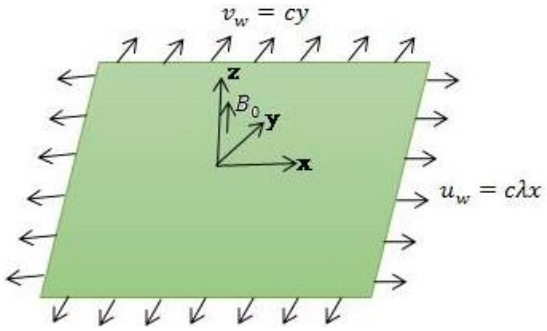

Fig. 1. Geometry of the problem.

3. Similarity solution

3.1. Fluid flow solution

Introducing the following similarity transformations to convert PDEs in to set of ODEs;

$$u = c\lambda x\, f'(\eta), v = cy[f'(\eta) + g'(\eta)],$$
$$w = -\sqrt{c\nu}[g(\eta) + (\lambda + 1)f(\eta)], \eta = \sqrt{\frac{c}{\nu}}z$$
$$u_p = c\lambda x F(\eta), v_p = cy[F(\eta) + G(\eta)], w_p = \sqrt{c\nu}[G(\eta) + (\lambda + 1)K(\eta)], \rho_r = \frac{\rho_p}{\rho} = H(\eta) \quad (10)$$

here, λ is the ratio of the velocities in y- and x-directions, and prime denote differentiation with respect to η.
Making use of Eq. (10), the equation of continuity is identically satisfied and momentum Eqs. (1-5) take the following form:

$$f''' + [g + (\lambda + 1)f]f'' - f'^2\lambda + \beta(F - f')H - Mf' = 0, \quad (11)$$

$$(f''' + g''') + [g + (\lambda + 1)f](f'' + g'') - (f' + g')^2 + \beta[(F + G) - (f' + g')] - [f' + g'] = 0, \quad (12)$$

$$[G + (\lambda + 1)K]F' + \lambda F^2 + \beta(F - f') = 0, \quad (13)$$

$$[F + G]^2 + [G + (\lambda + 1)K][F' + G'] + \beta[(F + G) - (f' + g')] = 0, \quad (14)$$

$$[G + (\lambda + 1)K][(\lambda + 1)K' + G'] + \beta\,[G + g + (\lambda + 1)(K + f)] = 0, \quad (15)$$

$$[G + (\lambda + 1)K]H' + [(\lambda + 1)(F + K') + G + G']H = 0. \quad (16)$$

The boundary conditions for the Eq. (8-9) are:

$$\eta = 0 : f' = 1, f = 0, g = g' = 0, \quad (17)$$

$$\eta \to \infty : \; f' = F = 0, g' = G = 0, K = -f - \frac{g}{\lambda+1}, H = \omega, \quad (18)$$

where $\beta = 1/c\tau_v$ is the fluid-particle intraction parameter, $H = \rho_p/\rho$ is the relative density, $M = \frac{\sigma B_0^2}{\rho_\tau}$ is the magnetic parameter, ω is the density ratio and its value is considered as 0.2 in this present study.

3.2. Heat transfer solution

To transform the energy equations into a nondimensional form, the dimensionless temperature profile for the clean and dusty fluids are introduced as follows:

$$\theta(\eta) = \frac{T - T_\infty}{T_f - T_\infty}, \theta_p(\eta) = \frac{T_P - T_\infty}{T_f - T_\infty} \quad (19)$$

where T_f and T_∞ denote the temperatures at the wall and large distance from the wall, respectively. Making use of Eq. (10 and 19) into Eq. (6 and 7), the energy equation takes the following form:

$$\theta'' + \Pr[g + (\lambda + 1)f]\,\theta' + Pr\beta_\tau[\theta_p - \theta]H + Pr\beta[Ec_x(F - f')^2 + Ec_y(F - f' + G - g')^2]H = 0, \quad (20)$$

$$[G + (\lambda + 1) + K]\theta_p' + \frac{c_p}{c_m}\beta_\tau[\theta_p - \theta] = 0, \quad (21)$$

where $Pr = \frac{\mu c_p}{k}$ is the Prandtl number, $Ec_x = \frac{(u_w)^2}{(T_f - T_\infty)c_p}$ and $Ec_y = \frac{(v_w)^2}{(T_f - T_\infty)c_p}$ are the Eckert numbers, and $\beta_T = \frac{1}{\tau_T c}$ is the fluid-particle interaction parameter for the temperature. The boundary conditions for the Eqs. (20 and 21) are:

$$\eta = 0 : \theta' = -B_i(1 - \theta), \quad (22)$$

$$\eta \to \infty : \theta_p = \theta = 0. \quad (23)$$

where $B_i = \sqrt{\frac{\nu}{c}}\frac{h_f}{k}$ is the Biot number.
The wall shear stress is given by:

$$\tau_{zx} = -\mu\left(\frac{\partial u}{\partial z} + \frac{\partial w}{\partial x}\right)_{z=0}, \tau_{zy} = -\mu\left(\frac{\partial v}{\partial z} + \frac{\partial w}{\partial y}\right)_{z=0} \quad (24)$$

The friction factor is written as:

$$Cf_x Re_x^{\frac{1}{2}} = -f''(0), Cf_y Re_y^{\frac{1}{2}} = -g''(0) \quad (25)$$

The surface heat transfer rate is given by:

$$q_w = -k\left(\frac{\partial T}{\partial y}\right)_{z=0} \quad (26)$$

The local Nusselt number is written as:

$$NuRe_x^{-\frac{1}{2}} = -\theta'(0) \quad (27)$$

4. Numerical solution

Reduced nonlinear ordinary differential Eqs. (11-16) and Eqs. (20 and 21) subjected to the associated boundary conditions are solved numerically using Runge–Kutta Fehlberg

fourth-fifth order method along with shooting technique. In the first step, a set of nonlinear ordinary differential Eqs. (1 -7) with boundary conditions Eq. (8 and 9) are discretized to a system of simultaneous differential equations of the first order by introducing new dependent variables.

$$f = y_1,\ y_1' = y_2,\ y_2' = y_3, y_3' = y_4,\ g = y_5,\ y_5' = y_6, y_6' = y_7, F = y_8,\ y_8' = y_9, G = y_{10},\ y_{10}' = y_{11}, H = y_{12}, K = y_{13}, y_{13}' = y_{14}\ , \theta = y_{15},\ y_{15}' = y_{16},\ \theta_p = y_{17} \quad (28)$$

In view of Eq. (28), Eqs. (11-16) and Eqs. (20-21) take the following forms:

$$y_3' = y_2^2\lambda - \beta(y_8 - y_2)y_{12} + My_2 - [y_5 + (\lambda+1)y_1]\ y_3, \quad (29)$$

$$y_7' = (y_2 + y_6)^2 - y_4 - [y_5 + (\lambda+1)y_1](y_3 + y_7) - \beta[(y_8 + y_{10}) - (y_2 + y_6)] + M[y_2 + y_6], \quad (30)$$

$$y_8' = -\frac{1}{[y_{10}+(\lambda+1)y_{13}]}[\lambda {y_8}^2 + \beta(y_8 - y_2)], \quad (31)$$

$$y_{10}' = -\frac{1}{[y_{10}+(\lambda+1)y_{13}]}\{\beta[(y_8 + y_{10}) + (y_2 + y_6)] + (y_8 + y_{10})^2\} - y_8', \quad (32)$$

$$y_{13}' = -\frac{1}{(\lambda+1)}\left\{\frac{1}{[y_{10}+(\lambda+1)y_{13}]}\ \beta[y_{10} + y_5 + (\lambda+1)(y_{13} + y_1)] + y_{11}\right\}, \quad (33)$$

$$y_{12}' = -\frac{1}{[y_{10}+(\lambda+1)y_{13}]}[(\lambda+1)(y_8 + y_{14}) + y_{10} + y_{11}]y_{12}, \quad (34)$$

$$y_{16}' = -\Pr\{[y_5 + (\lambda+1)y_1]y_{16} + \beta_\tau[y_{17} - y_{15}]y_{12} + \beta\left[Ec_x(y_8 - y_2)^2 + Ec_y(y_8 - y_2 + y_{10} - y_6)^2\right]y_{12}\}, \quad (35)$$

$$y_{17}' = -\frac{1}{[y_{10}+(\lambda+1)+y_{13}]}\frac{c_p}{c_m}\beta_\tau[y_{17} - y_{15}], \quad (36)$$

with the corresponding boundary conditions of:

$$y_1 = 0, y_2 = 1,\ y_5 = 0, y_6 = 0, y_{16} = -Bi(1 - y_{15}) \ \text{ at } \ \eta = 0, \quad (37)$$

$$y_2 = y_6 = 0, y_8 = y_{10} = 0, y_{13} = -y_1 - \frac{y_5}{\lambda+1}, y_{12} = \omega, y_{15} = y_{17} = 0 \text{ as } \eta \to \infty \quad (38)$$

To solve the Eqs. (29-36), the authors guess missed values which are not given at the initial conditions. Afterward, a finite value for η_∞ is chosen in such a way that all the far field boundary conditions are satisfied asymptotically. The bulk computations are considered with the value at η_∞= 5, which is sufficient to achieve the far field boundary conditions asymptotically for all values of the parameters considered. For the present problem, the authors took the step size $\Delta\eta = 0.001, \eta_\infty = 5$ and accuracy to the fifth decimal places. The CPU running time for existing numerical solution is 0.03 sec.

5. Results and discussion

In this section, the effect of magnetic parameter (M), fluid particle interaction parameter for velocity (β), the fluid velocity ratio (λ), the thermal fluid-particle interaction parameter (β_T), Biot number (B_i), Eckert number (Ec), Prandtl number (Pr) on the velocity and temperature fields are presented. The effect of velocity ratio λ on the velocity profiles $(f', f' + g')$ is shown in Fig. 2. From this figure, it can be seen that both f' and $f' + g'$ decrease with increasing λ values, and therefore the difference between the velocity components is larger and the velocity components (u, v) become the same.

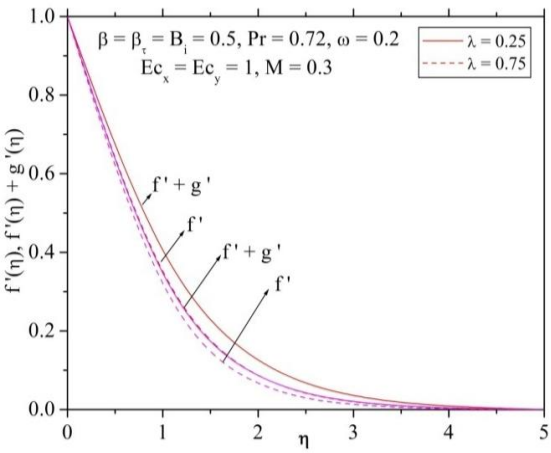

Fig. 2. Effect of velocity ratio, λ, on dimensionless velocity profiles f' and $(f' + g')$.

The dimensionless velocity profiles for different values of λ proportional to u and v velocity components are depicted in Figs. 3 and 4, respectively for both fluid and dust phase. As it

is seen, the behavior of the fluid phase $[f'(\eta), f'(\eta)+g'(\eta)]$ and dusty phase $[F(\eta), F(\eta)+G(\eta)]$ are the same and decreases with the increase in λ. It can also be seen that the fluid phase velocity is greater than the dust phase velocity and both are parallel.

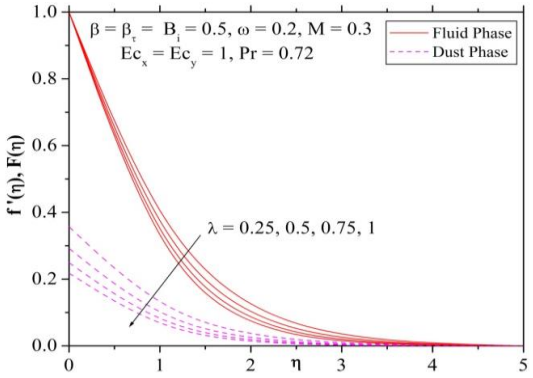

Fig. 3. Dimensionless profiles of u, u_p velocity components for different values of λ.

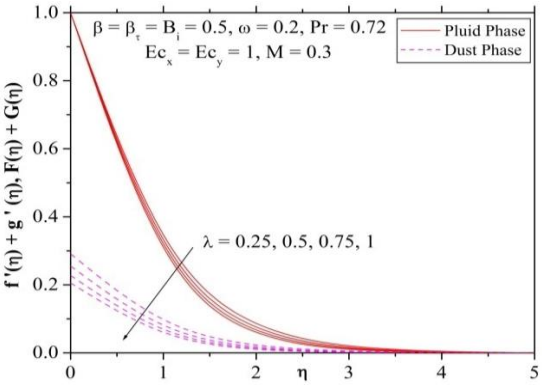

Fig. 4. Dimensionless profiles of v, v_p velocity components for different values of λ.

Figs. 5-7 shows the velocity and temperature profiles for various values of magnetic parameter. Here, $f'(\eta)$ represents the velocity in $x-$ direction while $[f'(\eta)+g'(\eta)]$ is the velocity in $y-$direction for the fluid phase, and $F(\eta)$ represents the velocity in $x-$direction while $[F(\eta)+G(\eta)]$ is the velocity in $y-$direction for the dust phase, respectively. It is observed that, the velocity profile decreases while the temperature profile increases with increasing M values. The effect of magnetic field on electrically conducting fluid results in a resistive type of force called Lorentz force which has a tendency to decrease the fluid velocity and to increase the temperature field. Due to this fact, the magnetic field effect has many possible control-based applications like in MHD ion propulsion, electromagnetic casting of metals, MHD power generation and etc.

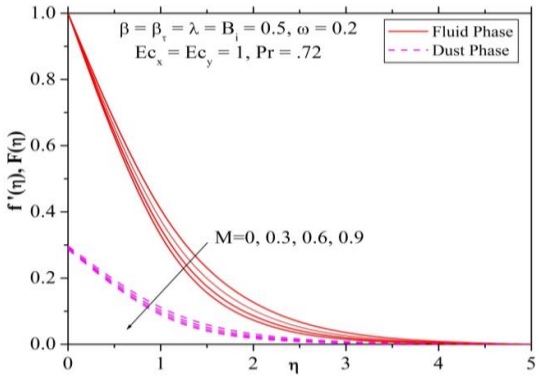

Fig. 5. Dimensionless profiles of u, u_p velocity components for different values of M.

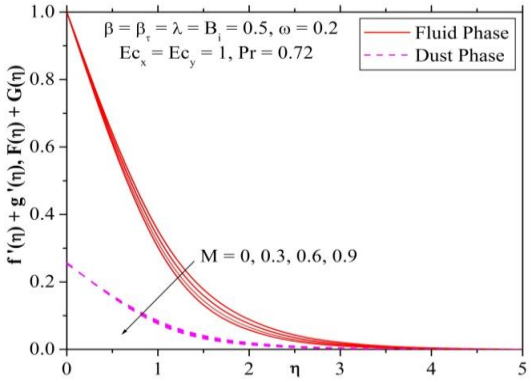

Fig. 6. Dimensionless profiles of v, v_p velocity components for different values of M.

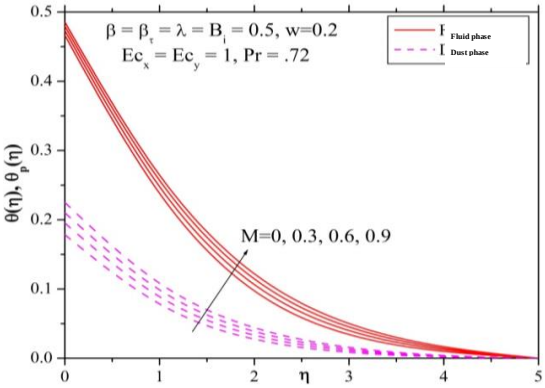

Fig. 7. Dimensionless temperature profiles for different values of M.

The influence of fluid-particle interaction parameter on velocity profile in both directions

for the fluid and dust phases are shown in Figs. 8 and 9. It is observed that with the increase in the fluid-particle interaction parameter, the thickness of momentum boundary layer decreases for fluid phase and, the opposite phenomena are observed in the dust phase, as shown in Figs. 8 and 9. From the figures, it is observed that the velocity decreases while the dust phase velocity increases with the increase in the values of β. Of course, the effect of variation of β is more sensible on the dusty phase than the fluid phase since the increase in β increases the contribution of particles of the fluid velocity, and so decreases the fluid velocity. This is evident because for the large values of $\beta(\tau \to o)$ the relaxation velocity time of the dusty fluid decreases, and therefore the velocities of both the fluid and dusty phases are the same. So, by increasing β, the velocity profiles of dusty and fluid phases are close to each other.

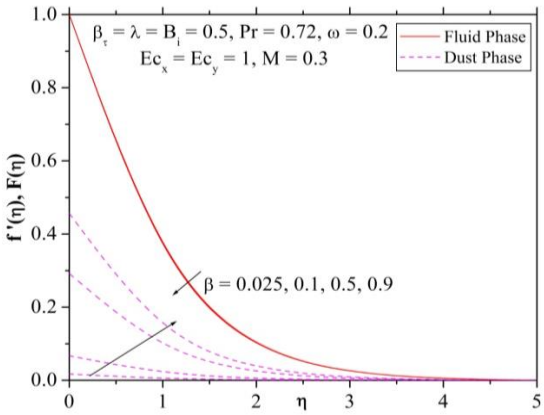

Fig. 8. Dimensionless profiles of u, u_p velocity components for different values of β.

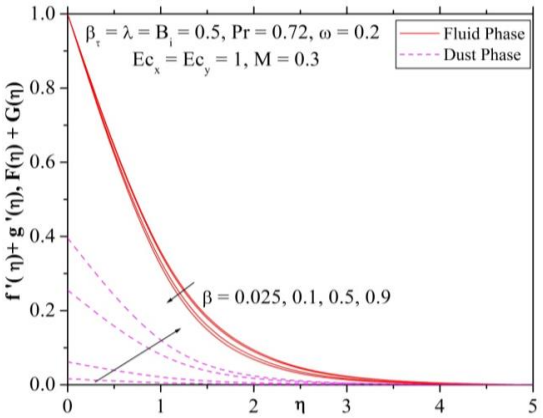

Fig. 9. Dimensionless profiles of v, v_p velocity components for different values of β.

The variation of dimensionless temperature profiles, θ, θ_p, for various values of λ, are presented in Fig. 10. As it is seen, the increase in λ causes the temperature profiles of both the dusty and fluid phases to decrease. Furthermore, one can observe from these figures that the values of the temperature are higher for the clean fluid than for the dusty fluid at all points, as excepted.

The variation of dimensionless temperature profiles for different values of the fluid and thermal particle interaction parameters β and β_T are presented in Figs. 11 and 12, respectively. It can be seen from Fig. 11 that the temperature of both the clean and dusty fluids decreases with increasing β and, of course, the effect of variation of β is more sensible on dusty phase than the fluid phase. This is because of the direct effect of β on velocity, and since the temperature depends on velocity, then the temperature varies with the variation of β.

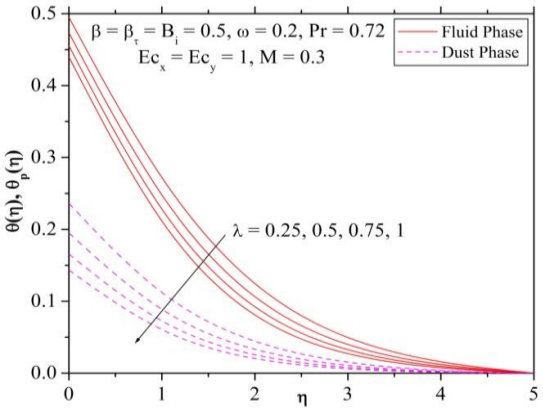

Fig. 10. Dimensionless temperature profiles for different values of λ.

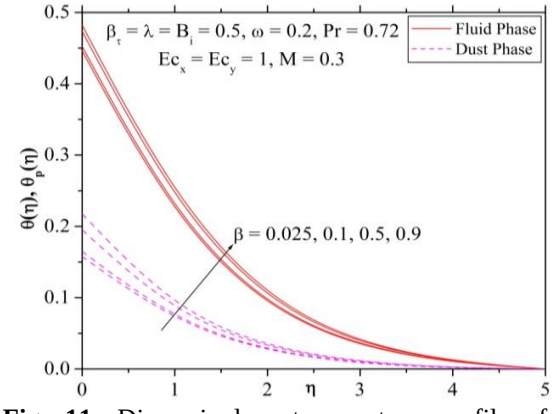

Fig. 11. Dimensionless temperature profiles for different values of β.

In Fig. 12, an adverse effect is found for the clean and dusty flows, as when β_T increases the clean fluid temperature, θ, decreases, whereas the dusty fluid temperature, θ_p, increases. This is similar to the trend of the velocity variation for different values of β (Figs. 8 and 9).

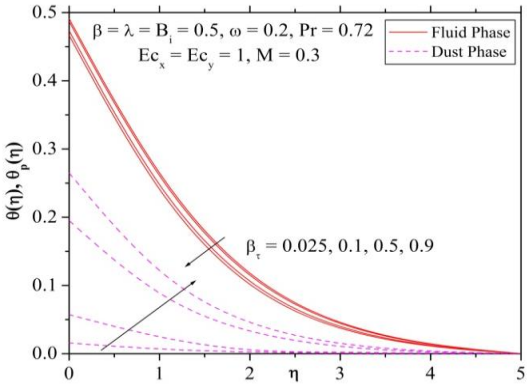

Fig. 12. Dimensionless temperature profiles for different values of β_T.

This is because for the large values of $\beta_T(\tau_T \to o)$, the thermal relaxation temperature time of the dusty fluid decreases, and then the temperatures of both the fluid and dusty phases are the same.

The effect of Eckert number (Ec) for temperature distribution is shown in Figs. 13 and 14. It is observed from the figures that the temperature profiles increases for both fluid and dust phases when the values of Ec increase. Eckert number expresses the relationship between the kinetic energy in the flow and the enthalpy. It embodies the conversion of kinetic energy into internal energy by work done against the viscous fluid stresses. The greater viscous dissipative heat causes a rise in the temperature and thermal boundary layer thickness for both fluid and particle phases. It is because heat energy is stored in the liquid due to frictional heating and this is true in both cases.

The effect of Prandtl number on heat transfer is shown in Fig. 15. The relative thickening of momentum and thermal boundary layers is controlled by Prandtl number (Pr). Since small values of Pr possess higher thermal conductivities so that the heat can diffuse from the sheet very quickly compared to the velocity. The figure reveals that the temperature decreases with the increase in the value of Pr. Hence Prandtl number can be used to increase the rate of cooling. Analyzing the graph reveals that the effect of increasing Pr decreases the temperature distribution in the flow region.

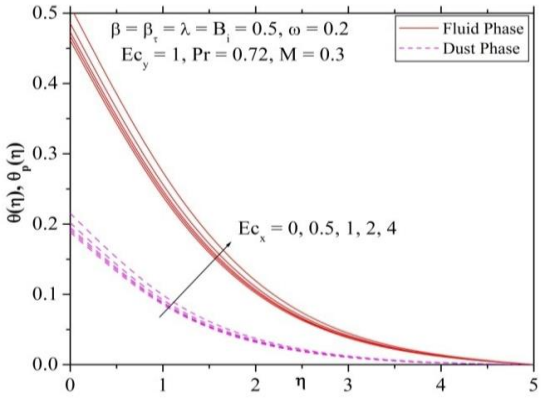

Fig. 13. Dimensionless temperature profiles for different values of Ec_X.

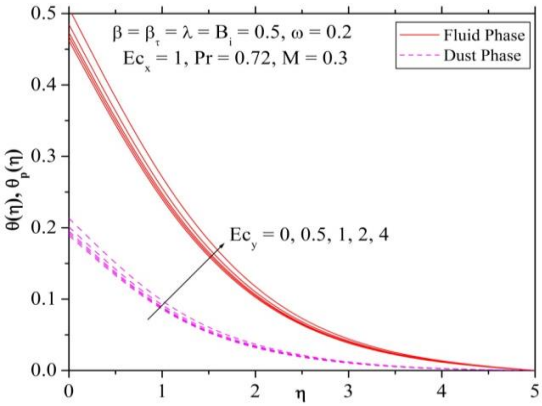

Fig. 14. Dimensionless temperature profiles for different values of Ec_y.

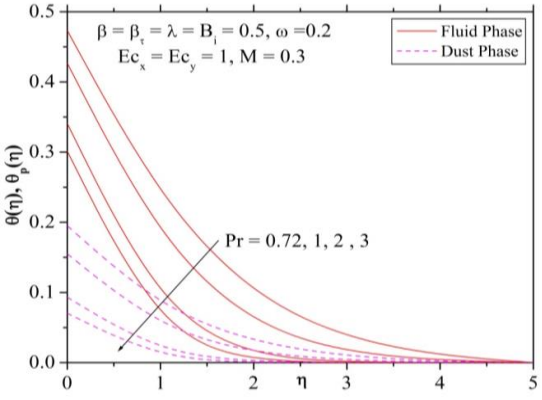

Fig. 15. Dimensionless temperature profiles for different values of Pr.

It is also evident that large values of Prandtl number result in thinning of the thermal boundary layer. From this figure, it is observed that both profiles decrease with increasing the Pr values. The influence of Biot number parameter, B_i, on the dimensionless temperature is displayed in Fig. 16. It shows that the dimensionless temperature profile increases with increasing Biot number. This is due to the fact that the convective heat exchange at the surface leads to enhance the thermal boundary layer thickness.

Figs. 17 and 18 show the magnitude of vector curve for fluid-particle interaction and magnetic parameters, respectively. Fig. 17 reveals that the magnitude of vector curve decreases with the increase in the value of β.

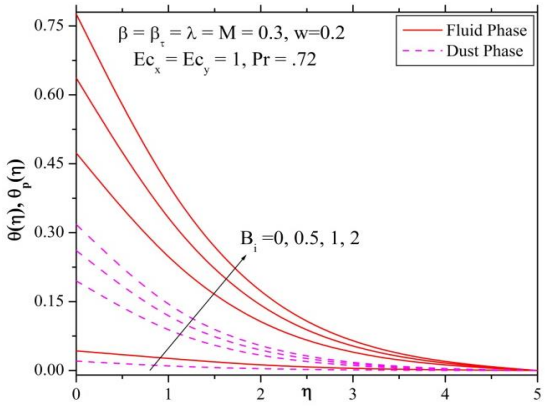

Fig. 16. Dimensionless temperature profiles for different values of B_i.

The same trend is observed in Fig. 18. The authors numerically studied the effects of Biot number, Eckert number, magnetic parameter, Prandtl number, fluid-particle interaction parameter for velocity, thermal fluid-particle interaction parameter and the fluid velocity ratio on skin friction and the local Nusselt number, which represents the heat transfer rate at the surface and are recorded in Table 1. It is clear that magnitude of both skin friction coefficient and the local Nusslet number decreases with increasing β, M and Ec. The local Nusselt number increases with Prandtl number and in consequence, increases the heat transfer rate at the surface. This is due to the fact that the higher Prandtl number reduces the thermal boundary layer thickness and increases the surface heat transfer rate. Also, high Prandtl number implies more viscous fluid which tends to retard the motion.

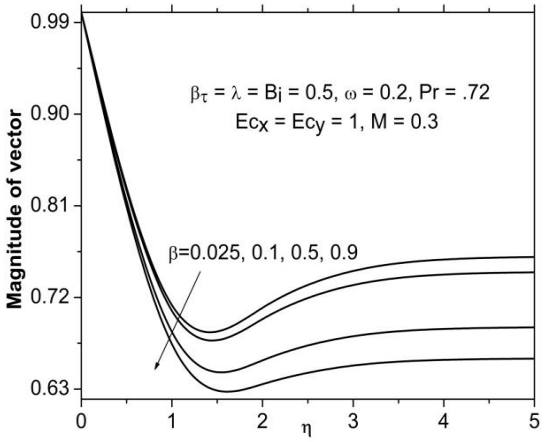

Fig. 17. Magnitude of vector curve for β.

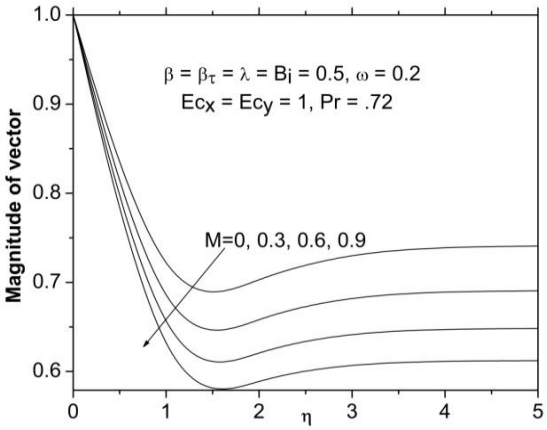

Fig. 18. Magnitude of vector curve for M.

6. Conclusions

In the present study, three-dimensional boundary layer flow and heat transfer of a dusty fluid toward a stretching sheet with convective boundary conditions are investigated. The governing boundary layer equations for the problem are reduced to dimensionless ordinary differential equations by a suitable similarity transformation. Numerical computations for the effects of controlling parameters on velocity and temperature fields are carried out. Some conclusions obtained from this investigation are summarized as follows:

- Fluid phase velocity is always greater than that of the particle phase.

Table 1. Values of skin friction coefficient and Nusselt number.

B_i	Ec_x	Ec_y	M	Pr	β	β_T	λ	$-f''(0)$	$-g''(0)$	$-\theta'(0)$
0	1	1	0.3	0.72	0.5	0.5	0.5	1.10259	0.26438	0
0.5								1.10259	0.26438	0.26332
1								1.10259	0.26438	0.36324
0.5	**0**							1.10259	0.26438	0.2694
	0.5							1.10259	0.26438	0.26636
								1.10259	0.26438	0.26332
		0						1.10259	0.26438	0.26899
		0.5						1.10259	0.26438	0.26615
		1						1.10259	0.26438	0.26332
			0					0.95862	0.29695	0.26677
			0.3					1.10259	0.26438	0.26332
			0.6					1.23046	0.24039	0.26015
				0.72				1.10259	0.26438	0.26332
				1.5				1.10259	0.26438	0.31307
				2				1.10259	0.26438	0.32954
					0.1			1.08283	0.17555	0.27385
					0.5			1.10259	0.26438	0.26332
					0.9			1.11486	0.31833	0.25899
						0.1		1.10259	0.26438	0.25653
						0.5		1.10259	0.26438	0.26332
						0.9		1.10259	0.26438	0.26674
							0.5	1.10259	0.26438	0.26332
							0.75	1.21505	0.1903	0.27236
							1	1.31707	0.12413	0.28017

- Increasing β value decreases fluid phase velocity and increases dust phase velocity.
- Increasing β_T value decreases fluid phase and increases dust phase of the temperature profile.
- Temperature profiles of fluid and dust phases increase with the increase of the Eckert number.
- Temperature profile increases β, B_i and decreases Pr.

Acknowledgments

Authors are thankful to University Grants Commission, New Delhi for providing financial support to pursue this work under a Major Research Project Scheme [F. No -43-419/2014(SR)].

References

[1] B. C. Sakiadis, "Boundary layer behaviour on continuous solid surface", *American Institute of Chemical Engineering Journal*, Vol. 7, pp. 26-28, (1961).

[2] L. J. Crane, "Flow past a stretching sheet", *Zeitschrift für angewandte Mathematik und Physik (ZAMP)*, Vol. 21, No. 4, pp. 645-647, (1970).

[3] I. C. Liu, H. H. Wanga and Y. F. Peng, "Flow and heat transfer for three-dimensional flow over an exponentially stretching surface", *Chemical Engineering Communications*, Vol. 200, No. 2, pp. 253-268, (2013).

[4] T. Hayat, B. Ashraf, S. A. Shehzad, and E. Abouelmagd, "Three-dimensional flow of Eyring Powell nanofluid over an exponentially stretching sheet", *International Journal of Numerical*

Methods for Heat and Fluid Flow, Vol. 25, No. 3, pp. 593-616, (2014).

[5] S. Nadeem, R. U. Haq, and N. S. Akbar, "MHD three-dimensional boundary layer flow of Casson nanofluid past a linearly stretching sheet with convective boundary condition", *IEEE Transactions on Nanotechnology*, Vol. 13, No. 1, pp. 109-115, (2014).

[6] M. H. Abolbashari, N. Freidoonimehr, F. Nazari, and M. M. Rashidi, "Entropy analysis for an unsteady MHD flow past a stretching permeable surface in nano-fluid", *Powder Technology*, Vol. 267, pp. 256-267, (2014).

[7] N. Freidoonimehr, M. M. Rashidi, and S.Mahmud, "Unsteady MHD free convective flow past a permeable stretching vertical surface in a nano-fluid", *International Journal of Thermal Sciences*, Vol. 87, pp.136-145, (2014).

[8] A. S. Butt, A. Ali, and A. Mehmood, "Study of flow and heat transfer on a stretching surface in a rotating Casson fluid", *Proceedings of the National Academy of Science (Springer)*, Vol. 85, No. 3, pp. 421-426, (2015).

[9] J. A. Khan, M. Mustafa, T. Hayat, and A. Alsaedi, "Three-dimensional flow of nanofluid over a non-linearly stretching sheet: An application to solar energy", *International Journal of Heat and Mass Transfer*, Vol. 86, pp.158-164, (2015).

[10] S. A. Shehzad, Z. Abdullah, F. M. Abbasi, T. Hayat, and A. Alsaedi, "Magnetic field effect in three-dimensional flow of an Oldroyd-B nanofluid over a radiative surface", *Journal of Magnetism and Magnetic Materials*, Vol. 399, pp.97-108, (2016).

[11] L. Kolsi, H. F. Oztop, A. Alghamdi, N. Abu-Hamdeh, A. Borjini, and H. B. A. Aissia, "Computational work on a three dimensional analysis of natural convection and entropy generation in nanofluid filled enclosures with triangular solid insert at the corners", *Journal of Molecular Liquids*, Vol. 218, pp. 260-274, (2016).

[12] T. Hayat, T. Muhammad, S. A. Shehzad, and A. Alsaedi, "On three-dimensional boundary layer flow of Sisko nanofluid with magnetic field effects", *Advanced Powder Technology*, Vol. 27, No. 2, pp. 504-512, (2016).

[13] T. Hayat, M. Mumtaz, A. Shafiq, and A. Alsaedi, "Thermal stratified three-dimensional flow with inclined magnetic field and Joule heating", *Journal of the Brazilian Society of Mechanical Sciences and Engineering*, Vol. 39, No. 5, pp. 1607-1621, (2017).

[14] P. G. Saffman, "On the stability of laminar flow of a dusty gas", *Journal of Fluid Mechanics*, Vol. 13, No. 1, pp. 120-128, (1962).

[15] K. M. Chakrabarti, "Note on boundary layer in a dusty gas", *American Institute of Aeronautics and Astronautics Journal*, Vol. 12, No. 8, pp. 1136-1137, (1974).

[16] N. Datta, and S. K. Mishra, "Boundary layer flow of a dusty fluid over a semi-infinite flat plate", *Acta Mechanica*, Vol. 42, No. 1-2, pp. 71-82, (1982).

[17] S. Mosayebidorcheh, M. Hatami, D. D. Ganji, T. Mosayebidorcheh, and S. M. Mirmohammadsadeghi, "Investigation of transient MHD couette flow and heat transfer of dusty fluid with temperature-dependent properties", *Journal of Fluid Mechanics*, Vol. 8, No. 4, pp. 921-929, (2015).

[18] O. M. Prakash, O. D. Makinde, D. Kumar, and Y. K. Dwivedi, "Heat transfer to MHD oscillatory dusty fluid flow in a channel filled with a porous medium", *Sadhana*, Vol. 40, No. 4, pp. 1273-1282, (2015).

[19] H. A. Attia, W. Abbas, A. E. D. Abdin, and M. A. M. Abdeen, "Effects of ion slip and hall current on unsteady couette flow of a dusty fluid through porous media with heat transfer", *High Temperature*, Vol. 53, No. 6, pp. 891-898, (2015).

[20] R. Muthuraj, K. Nirmala, and S. Srinivas, "Influences of chemical reaction and wall properties on MHD peristaltic transport of

a dusty fluid with heat and mass transfer", *Alexandria Engineering Journal*, Vol. 55, No. 1, pp. 597-611, (2016).

[21] S. Manjunatha, and B. J. Gireesha, "Effects of variable viscosity and thermal conductivity on MHD flow and heat transfer of a dusty fluid", *Ain Shams Engineering Journal*, Vol. 7, No. 1, pp. 505-515, (2016).

[22] M. R. Mohaghegh, and A. B. Rahimi, "Three–dimensional stagnation–point flow and heat transfer of a dusty fluid toward a stretching sheet", *Journal of Heat Transfer*, Vol. 138, No. 1, pp. 112001 (12 pages), (2016).

[23] V. W. J. Anand, S. Ganesh, A. M. Ismail, and C. K. Kirubhashankar, "Unsteady MHD dusty fluid flow of an exponentially stretching sheet with heat source through porous medium", *Applied Mathematical Sciences*, Vol. 9, No. 42, pp. 2083-2090, (2015).

[24] P. T. Manjunatha, B. J. Gireesha, and B. C. Prasannakumara, "Effect of radiation on flow and heat transfer of MHD dusty fluid over a stretching cylinder embedded in a porous medium in presence of heat source", *International Journal of Applied and Computational Mathematics*, Vol. 3, No. 1, pp. 293-310, (2017).

[25] B. C. Prasannakumara, B. J. Gireesha, and P. T. Manjunatha, "Melting phenomenon in MHD stagnation point flow of dusty fluid over a stretching sheet in the presence of thermal radiation and non-uniform heat source/sink", *International Journal for Computational Methods in Engineering Science and Mechanics*, Vol. 16, No. 5, pp. 265-274, (2015).

[26] M. M. Bhatti, A. Zeeshan, and R. Ellahi, "Study of heat transfer with nonlinear thermal radiation on sinusoidal motion of magnetic solid particles in a dusty fluid", *Journal of Theoretical and Applied Mechanics*, Vol. 46, No. 3, pp. 75-94, (2016).

[27] B. J. Gireesha, P. Venkatesh, N. S. Shashikumar, and B. C. Prasannakumara, "Boundary layer flow of dusty fluid over a permeable radiating stretching surface embedded in a thermally stratified porous medium in the presence of uniform heat source", *Nonlinear Engineering*, Vol. 6, No. 1, pp. 31-41, (2017).

[28] R. C. Bataller, "Radiation effects for the Blassius and Sakiadis flows with a convective surface boundary condition", *Applied Mathematics and Computation*, Vol. 206, No. 2, pp. 832-840, (2008).

[29] A. Aziz, "A similarity solution for laminar thermal boundary layer over a flat plate with a convective surface boundary condition", *Communications in Nonlinear Science and Numerical Simulation*, Vol. 14, No. 4, pp. 1064-1068, (2009).

[30] O. D. Makinde, "Similarity solution of hydromagnetic heat and mass transfer over a vertical plate with a convective surface boundary condition", *International Journal of Physical Sciences*, Vol. 5, No. 6, pp. 700-710, (2010).

[31] J. H. Merkin, and I. Pop, "The forced convection flow of a uniform stream over a flat surface with a convective surface boundary condition", *Communications in Nonlinear Science and Numerical Simulation*, Vol. 16, No. 9, pp. 3602-3609, (2011).

[32] G. K. Ramesh, B. J. Gireesha, and R. S. R. Gorla, "Boundary layer flow past a stretching sheet with fluid‑particle suspension and convective boundary condition", *Heat Mass Transfer*, Vol. 51, No. 8, pp.1061-1066, (2015).

[33] M. H. Abolbashari, N. Freidoonimehr, F. Nazari, and M. M. Rashidi, "Analytical modeling of entropy generation for Casson nano-fluid flow induced by a stretching surface", *Advanced Powder Technology*, Vol. 26, No. 2, pp. 542-552, (2015).

[34] R. Kandasamy, C. Jeyabalan, and K. K.S. Prabhu, "Nanoparticle volume fraction with heat and mass transfer on MHD mixed convection flow in a nanofluid in the presence of thermo-diffusion under convective boundary condition", *Applied*

Nanoscience, Vol. 6, No. 2, pp. 287-300, (2016).

[35] M. R. Krishnamurthy, B. C. Prasannakumara, R. S. R. Gorla, and B. J. Gireesha, "Non-linear thermal radiation and slip effect on boundary layer flow and heat transfer of suspended nanoparticles over a stretching sheet embedded in porous medium with convective boundary conditions", *Journal of Nanofluids*, Vol. 5, No. 4, pp. 522-530, (2016).

[36] T. Hayat, S. Makhdoom, M. Awais, S. Saleem, and M. M. Rashidi, "Axisymmetric Powell-Eyring fluid flow with convective boundary condition: optimal analysis", *Applied Mathematics and Mechanics*, Vol. 37, No. 7, pp. 919-928, (2016).

[37] N. Freidoonimehr, and M. M. Rashidi, "Analytical approximation of heat and mass transfer in MHD non-Newtonian nanofluid flow over a stretching sheet with convective surface boundary conditions", *International Journal of Biomathematics*, Vol. 10, No. 1, pp. 1750008 (25 pages), (2017).

How to cite this paper:

B. C. Prasannakumara, N. S. Shashikumar and M. Archana"Three-dimensional boundary layer flow and heat transfer of a dusty fluid towards a stretching sheet with convective boundary conditions" *Journal of Computational and Applied Research in Mechanical Engineering,* Vol. 8, No. 1, pp. 25-38, (2018).

DOI: 10.22061/jcarme.2017.2401.1227

URL: http://jcarme.sru.ac.ir/?_action=showPDF&article=774